Journal of Materials Science & Technology 34 (2018) 1273–1280

Contents lists available at ScienceDirect

Journal of Materials Science & Technology

journal homepage: www.jmst.org

Structural design of Cr/GLC films for high tribological performance in artificial seawater: Cr/GLC ratio and multilayer structure

Lei Li[a,b], Peng Guo[a], Lin-Lin Liu[a], Xiaowei Li[a], Peiling Ke[a,*], Aiying Wang[a,*]

[a] Key Laboratory of Marine Materials and Related Technologies, Zhejiang Key Laboratory of Marine Materials and Protective Technologies, Ningbo Institute of Materials Technology and Engineering, Chinese Academy of Sciences, Ningbo 315201, China
[b] University of Chinese Academy of Sciences, Beijing 100049, China

ARTICLE INFO

Article history:
Received 20 April 2017
Received in revised form 5 June 2017
Accepted 8 June 2017
Available online 8 December 2017

Keywords:
Cr/GLC films
Multilayer
Modulation ratio
Tribological properties

ABSTRACT

In this paper, graphite-like carbon (GLC) films with Cr buffer layer were fabricated by DC magnetron sputtering technique with the thickness ratio of Cr to GLC films varying from 1:2 to 1:20. The effect of Cr/GLC modulation ratio on microstructure, mechanical and tribological properties in artificial seawater was mainly investigated by scanning electron microscopy (SEM), energy dispersive spectroscopy (EDS), nano-indenter and a reciprocating sliding tribo-meter. The propagation of defects plays an important role in the evolution of delamination, which is critical to wear failure of GLC films in artificial seawater. Designing the proper multilayer structure could inhibit the defects propagation and thus protect the basis material. The multilayer Cr/GLC film with optimized ratio of 1:3 demonstrates a low average friction coefficient of 0.08 ± 0.006 and wear rate of $(2.3 \pm 0.3) \times 10^{-8}$ mm^3/(N m) in artificial seawater, respectively.

1. Introduction

Nowadays, some conclusive frictional components of marine equipment, such as pump, cylinder piston, bearing and propeller, have been widely used and serviced in seawater environment directly with the development of marine economy [1]. To achieve the safety, reliability and long service life of marine equipment, it is critical to enhance the comprehensive properties of frictional components in marine systems [2]. An effective method is to prepare availably protective films on the surface of frictional components [3–5]. Among all protective and lubricating films, amorphous carbon films combining excellent chemical and physical natures (good stability, ideal hardness and seductive anti-wear capacity) are becoming the best candidate to solve above-mentioned problems [6].

According to previous reports, amorphous carbon (a-C) films consisting of sp^2- and sp^3-bonded can divide into DLC and GLC films. GLC film with significant sp^2-hybridized carbon and its unique combination of desirable properties, including low friction coefficient, high hardness and chemical inertness have been widely used in the surface engineering field over the past few decades [7,8]. The favorable intrinsic properties make the GLC film well applicable in the marine frictional components as a protective layer to improve the tribological performance for the moving parts operated in seawater [9]. However, the insufficient adhesion strength often leads to flake and peel off from the substrate, thus limiting its practical application [10,11]. Moreover, through-thickness defects accompanied with film deposition usually resulted in the inward penetration of corrosive species to the substrate, leading to deteriorative corrosion resistance and tribological properties [12]. Functional buffer layer addition [12–15] and multilayer structural design [12,16,17] are two effective strategies for overcoming these problems and improving the tribological properties. Ti and Cr are the most widely used metallic candidates for the design of buffer layer [18,19]. In a very recent work, Wang et al. [20] showed that Cr buffer layer could improve adhesion strength and tribological performance of GLC films, which is consistent with the work of Stallard et al. [21], who found that the Cr/GLC films showed low coefficient frictions and wear rates in air, water and oil environments at high loads. Wang et al. [22] revealed that the long-term mechanical stress and corrosion attack could be avoided by the multilayer diamond-like carbon film. Bai et al. [16] studied the corrosion and tribological performances of amorphous carbon (a-C) coated Ti_6Al_4V alloy in Hank's solution and confirmed that a-C multilayer films exhibited enhanced wear and corrosion resistance simultaneously compared with the a-C single-layer film. Despite corrosive and tribological

* Corresponding authors.
E-mail addresses: kepl@nimte.ac.cn (P. Ke), aywang@nimte.ac.cn (A. Wang).

https://doi.org/10.1016/j.jmst.2017.12.002
1005-0302/

Table 1
Deposition parameters of the Cr/GLC films.

Films	Modulation ratio R	Deposition time (Cr buffer layer)	Deposition time (GLC films)
Cr/GLC-S1	1: 2	20 min	107 min
Cr/GLC-S2	1: 3	15 min	120 min
Cr/GLC-S3	1: 5	10 min	150 min
Cr/GLC-S4	1: 10	5 min	154 min
Cr/GLC-S5	1: 20	3 min	155 min

Table 2
Deposition parameters of the multilayer Cr/GLC films.

Modulation ratio, *R*	Deposition time (Cr buffer layer)	Deposition time (GLC films)
1:3	5 min (repeat for 3 times)	40 min (repeat for 3 times)

performances can be greatly improved by multilayer structure, the relationship between multilayer structural parameters (e.g., modulation period and modulation ratio) and its protective performances is unclear and does not attract much attention till now, which is crucial for the multilayer design in the seawater.

In this work, graphite-like carbon films with Cr buffer layer in different modulation ratio (Cr: GLC = 1:2, 1:3, 1:5, 1:10, 1:20) were fabricated by direct current magnetron sputtering technique. Then the structure and corresponding tribological properties in artificial seawater were investigated. The influence of Cr/GLC modulation ratio and the effect of multilayer structure on tribological performance in seawater were studied. Tribological mechanism of the Cr/GLC films in seawater was discussed in terms of the structure, mechanical, and tribological behaviors. It is expected that the proper modulation ratio and multilayer structure design can improve corrosive and tribological performance in seawater and thus protect the basis material from corrosion and wear.

2. Experimental

2.1. Film preparation

The Cr/GLC films were fabricated by direct current magnetron sputtering technique. P-type Si (100) wafers and mirror-finished 316L austenitic stainless steels with dimension of 20 mm × 20 mm × 1 mm were used as substrates. All substrates were ultrasonically cleaned in acetone, ethanol in succession and dried in air blow. The distance from the substrates to the targets was 10 cm. Before deposition, the chamber was evacuated to a vacuum of 4.0×10^{-3} Pa with a molecular pump assisted with a mechanical pump. Then the substrates were etched and pre-cleaned for 30 min using Ar+ plasma glow with substrates bias voltages of −350 V. During film deposition process, the Ar flow rate was kept at 50 sccm. Then the Cr buffer layers were first deposited on the substrates followed by the GLC layers. Deposition of the Cr layer was kept under a bias voltage of −100 V, a target current of 3.0 A. Sputtering graphite target was set as 3.0 A and bias voltage was conducted as −200 V. Five kinds of Cr/GLC films having different thickness ratio [Cr: CLC = 1:2 (S1), 1:3 (S2), 1:5 (S3), 1:10 (S4), 1:20 (S5)] were deposited as shown in Table 1. Then the deposition steps of Cr and GLC layers were setup as one block. The block was repeated for 3 times to form the multilayer Cr/GLC film. Deposition conditions are listed in Table 2.

2.2. Film characterization

The Hitachi S4800 high-resolution field emission SEM was used to analyze the cross-sectional morphology of the Cr/GLC films. The carbon atomic bonds of the GLC films were analyzed by

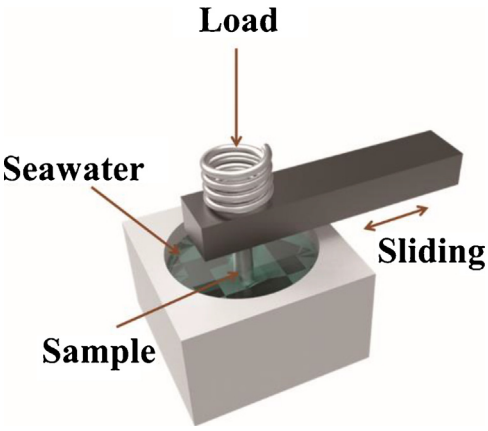

Fig 1. Schematic diagram of tribological setup.

Table 3
Chemical composition of artificial seawater (g/L).

NaCl	$MgCl_2$	Na_2SO_4	$CaCl_2$	KCl	$NaHCO_3$	KBr	H_3BO_3	$SrCl_2$	NaF
24.53	5.20	4.09	1.16	0.695	0.201	0.101	0.027	0.025	0.003

Raman spectrum (Renishaw inVia-reflex) with a 532 nm laser. The nano-indenter (MTS-G200) was applied to characterize mechanical properties by a continuous stiffness measurement mode. High-resolution transmission electron microscopy (HRTEM, Tecnai F20), which was conducted at 200 kV with a resolution of 0.24 nm, was used to study the microstructure of the Cr/GLC films in cross-section. The specimens for TEM examination were prepared by mechanical thinning and ion milling. Tribological tests of the Cr/GLC films in artificial seawater were conducted by using a reciprocating ball-on-disk tribo-meter (RTEC MFT5000) with commercial Si_3N_4 balls (6 mm in diameter) loaded at 5 N, which have high hardness and good corrosion resistance in seawater. The schematic view of components of tribological tester is shown in Fig. 1. The sliding velocity and frequency were set as 0.02 m/s and 2 Hz, respectively. The sliding time was 3600 s totally. The artificial seawater was made up according to the ASTM 1141-98 standard as shown in Table 3 [23]. After the tribo-tests, wear track profiles of the Cr/GLC films were measured by surface profilometer (Alpha Step-IQ). The wear rate was calculated by the following equation:

$$W = V/(F \times L) \quad (1)$$

where V is the wear loss of the film in m^3, F is the normal load applied in N and L is the sliding distance in m totally [24].

The SEM morphologies of wear tracks were characterized by field emission scanning electron microscope (FE-SEM, FEI Quanta FEG 250). The 3D worn morphology coupled Si_3N_4 balls were analyzed by using laser scanning confocal microscopy (LSCM, Keyence VK-X200 K).

3. Results and discussion

3.1. Microstructural characterization

Fig. 2 shows the cross-sectional microstructure of the Cr/GLC films. All the films are with different modulation ratio (R is from 1:2 to 1:20) and have an overall thickness of ~1.0 μm. The films are consists of Cr buffer layer and GLC film, which present clear interface and good bond to the substrate, turning out the structure and modulation ratio can be accurately controlled. The buffer layers of S1, S2, S3, and S4 exhibit weak columnar structures [25], while the S5 displays no obvious columnar crystals because of the thinner thickness.

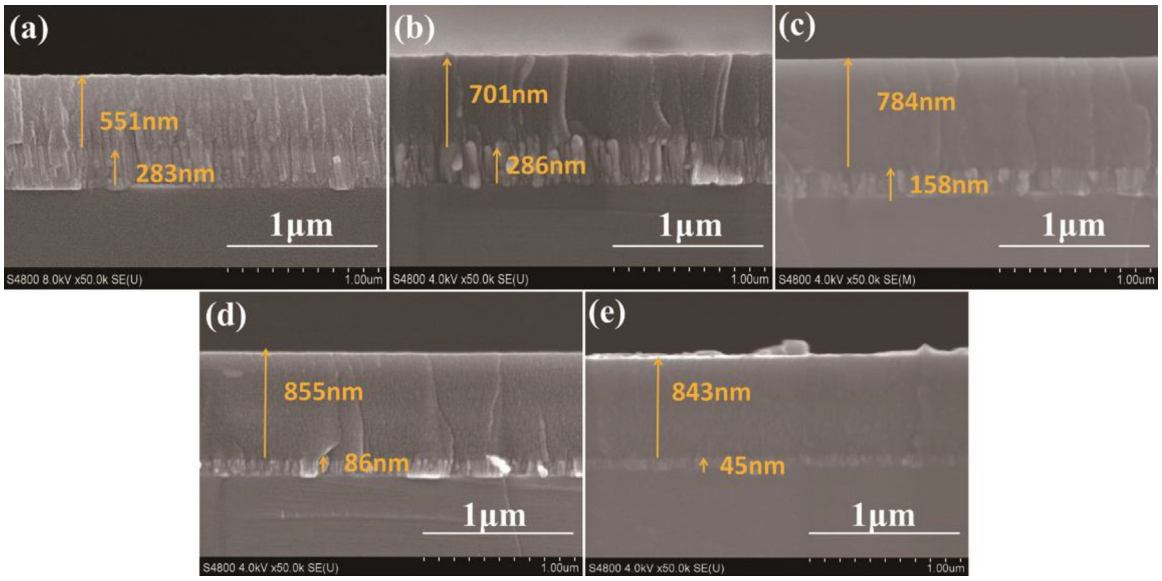

Fig. 2. Cross-sectional morphologies of the Cr/GLC films with different modulation ratio: (a) Cr/GLC-S1, (b) Cr/GLC-S2, (c) Cr/GLC-S3, (d) Cr/GLC-S4, (e) Cr/GLC-S5.

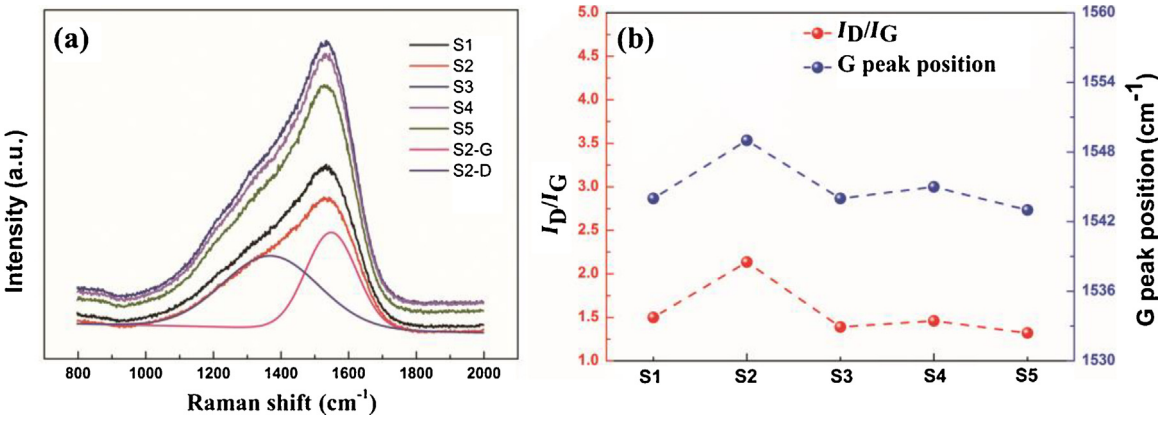

Fig. 3. (a) Raman spectra and (b) fitted G peak position, I_D/I_G of the Cr/GLC films with different modulation ratio.

Raman spectroscopy is a nondestructive technique to investigate the microstructure of carbonaceous films. Fig. 3(a) shows the Raman spectra of different modulation ratio monolayer films. The Raman spectra acquired from different samples can be fitted into two Gaussian peaks: D and G peaks, which is around 1380 and 1568 cm^{-1}, respectively [26]. The two peaks are both caused by sp^2 structure, wherein the *G* peak corresponds to sp^2 cluster structure, from the "stretching" vibration of the carbon ring and C—C bonds in the carbon chain; while the D peak corresponds to disorderly small sp^2 graphite structure, from "breathing" vibrations of the carbon ring [27]. The changes of strength ratio of obtained D peak and G peak (I_D/I_G), as well as G peak position (position (G)) after Gaussian fitting can indirectly reflect the carbon atomic structure, as shown in Fig. 3(b). With increasing the modulation ratio, the I_D/I_G and position (G) increase from S1 to S2 and then decrease to stable values; when the modulation ratio is 1:3, the maximal values of I_D/I_G and G peak position reach 2.13 and 1549 cm^{-1}. With the increase of graphitic component in the GLC film, it is empirically known that the I_D/I_G increases and G peak position shifts upwards [28]. Compared with other modulation ratio, the Cr/GLC film with modulation ratio of 1:3 has the most content of sp^2. Previous researches have proposed that metal buffer layer serve as catalysts in the formation of sp^2 structures, while the effect of the metal buffer thickness is uncertain [29,30].

In order to characterize the microstructure, the cross-sectional HRTEM (high resolution transmission electron microscopy) micrographs and the corresponding SAED (selected area electron diffraction) of the Cr/GLC film with modulation ratio of 1:2 are shown in Fig. 4. Clearly, the SAED in Fig. 4(b) indicates a typical amorphous structure with a broad and diffuse diffraction halo [31]. The Cr buffer layer shows typical columnar grain growth trends and the interlocked structure with amorphous carbon layer. It played an important role in enhancing the tribological performance of the Cr/GLC films [32].

3.2. *Mechanical properties of the Cr/GLC films*

Generally speaking, good mechanical properties of films, such as high hardness and toughness, will benefit for a great wear-resistant property. The hardness and elastic modulus of the Cr/GLC films are presented in Fig. 5. As shown in the figure, the nano-hardness and elastic modulus of the Cr/GLC film firstly decrease and then increase with increasing Cr/GLC modulation ratio, and the lowest hardness and elastic modulus of 16.0 ± 0.7 GPa and 154.3 ± 9.8 GPa are obtained for the Cr/GLC film with modulation ratio of 1:3, which are close to previous studies by Zhang et al. [33]. It is noted that the mechanical properties of the Cr/GLC films result from the sp^3 hybridized carbon content. Depending on the Raman results,

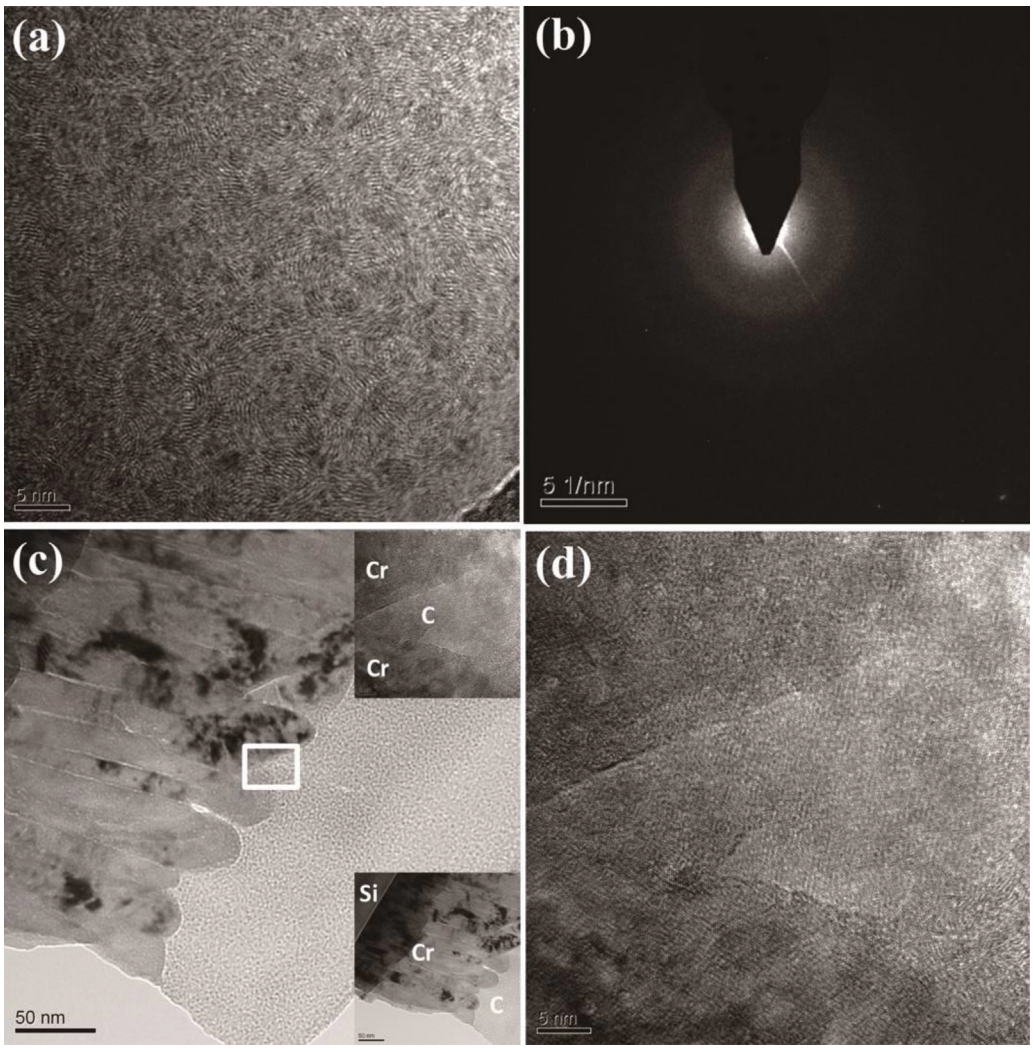

Fig. 4. Cross-sectional HRTEM (high-resolution transmission electron microscopy) micrographs of Cr/GLC-S1 and the corresponding SAED (selected area electron diffraction) of the carbon layer.

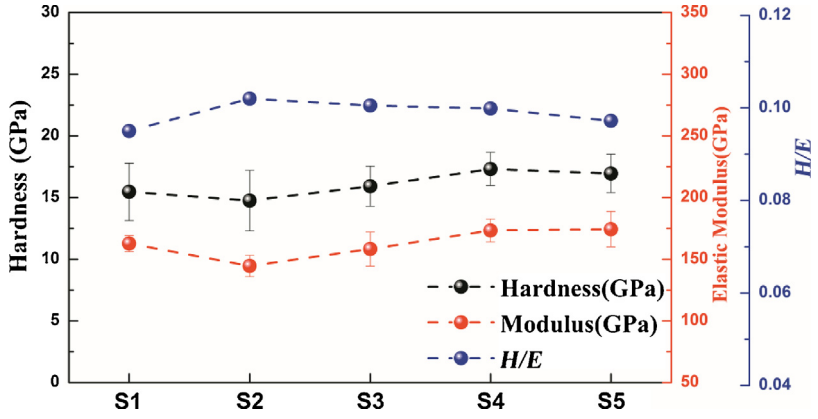

Fig. 5. Mechanical properties of the Cr/GLC films with different modulation ratio.

the graphitization degree tends to be higher as the modulation ratio change from 1:2 to 1:3, leading to the obvious reduction of hardness. Hardness has long been regarded as an important material property affecting wear resistance [34], but it is also being recognized that the elasticity and toughness of the films can be equally important parameters of wear resistance. The elastic behavior of films is described by the *H/E* ratio. According to Leyland and Matthews [34], the *H/E* ratio can be served as a reference for evaluating the tribological behavior of coating materials: i.e., the higher the *H/E* ratio, the higher the wear resistance. From Fig. 5, the Cr/GLC film with modulation ratio of 1:3 shows the highest *H/E* ratio, which can account for its high tribological performance.

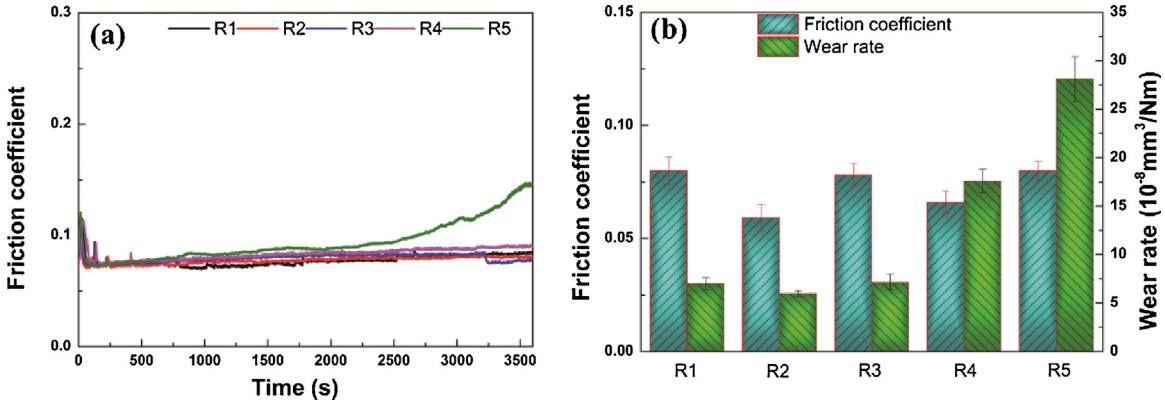

Fig. 6. (a) Friction coefficient curves of the Cr/GLC films sliding against Si_3N_4 balls in artificial seawater and (b) The average friction coefficients and wear rates of the Cr/GLC films.

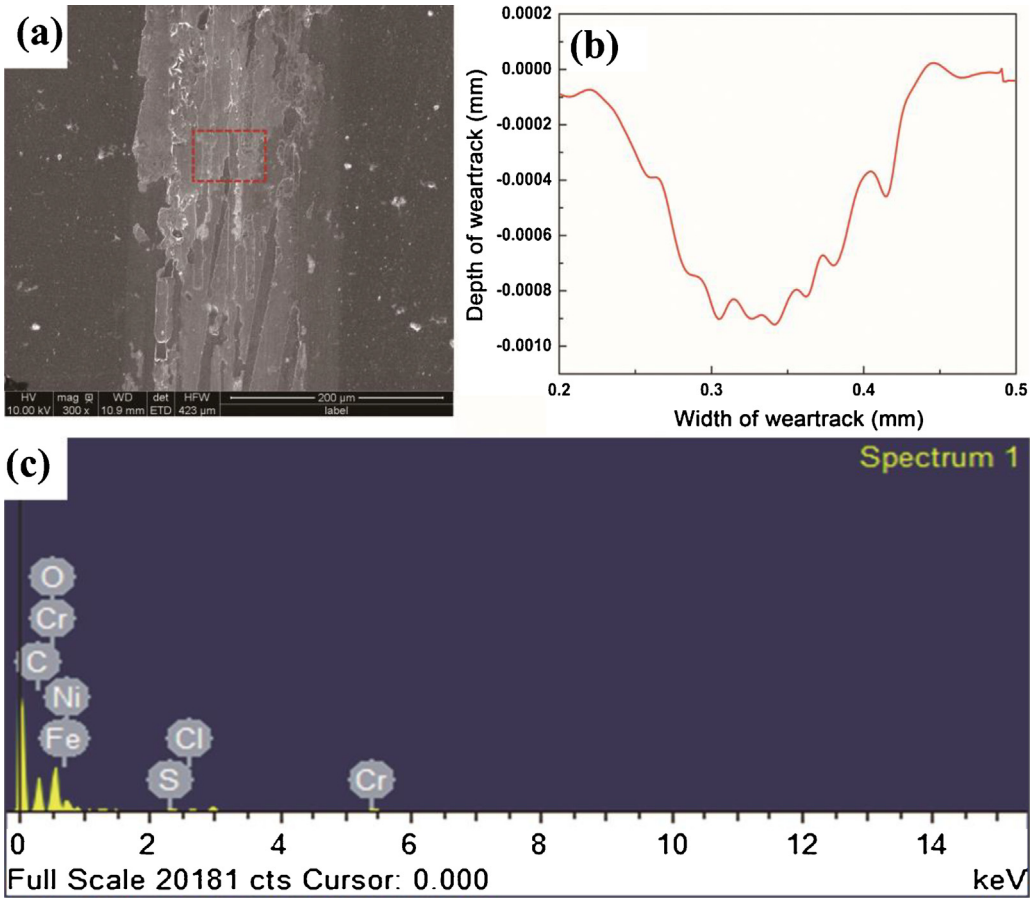

Fig. 7. Wear track of the Cr/GLC film with the modulation ratio of 1:3. (a) surface morphology, (b) 2D profile, (c) EDS analysis.

3.3. *Friction and wear behaviors of the Cr/GLC films in seawater*

To characterize the tribological performance of Gr/GLC films in seawater, the friction coefficient curves of the monolayer Cr/GLC films sliding against Si_3N_4 balls in seawater are shown in Fig. 6(a). It can be found that the friction coefficients in seawater are less than 0.1. The friction curves of the Cr/GLC films are characterized by two different stages: (1) an initial decrease from a high value to 0.075 with 100 s; (2) a subsequent gradual increase to a stage which remains for the test period with minor fluctuations. In order to search the differences of the friction behaviors, average friction coefficients and wear rates of the Cr/GLC films in artificial seawater are calculated as shown in Fig. 6(b). The values of the average friction coefficients are calculated by averaging the values of the experimental data after 100 s. Based on Fig. 6(a) and (b), low friction coefficients ranging from 0.059 to 0.092 of the Cr/GLC films in seawater are clearly seen, demonstrating the out-standing self-lubricating behaviors in seawater. The friction coefficients of the Cr/GLC films with modulation ratio of 1:2 and 1:3 are slightly lower than those of the Cr/GLC films with modulation ratio of 1:5, 1:10 and 1:20, while the Cr/GLC film with modulation ratio of 1:3 exhibits the smallest friction coefficient than any other films. It is well accepted that high sp^2 content can promote the graphitization of a lubricant transfer film at the contact surface. Therefore, the high sp^2 content of Cr/GLC film with modulation of 1:3 can account for the results, which has impact on the graphitization of tribo-film formed on

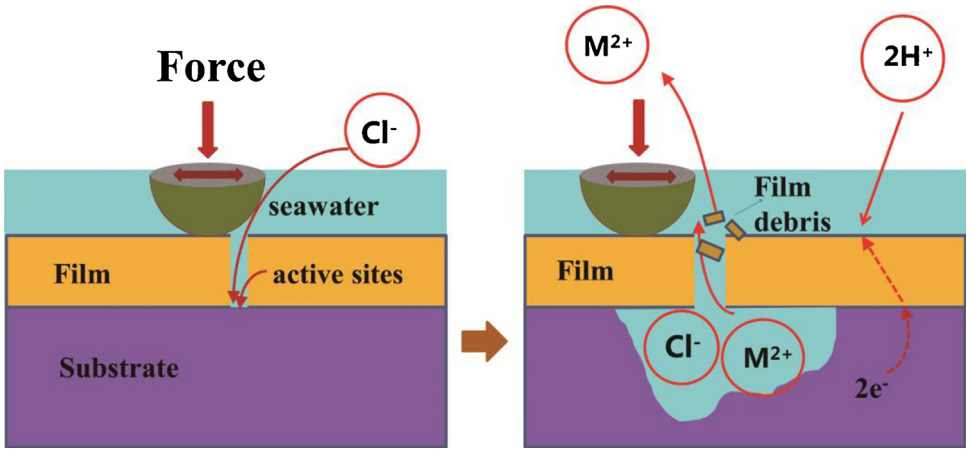

Fig. 8. Schematic images of wear behavior of the Cr/GLC films in seawater.

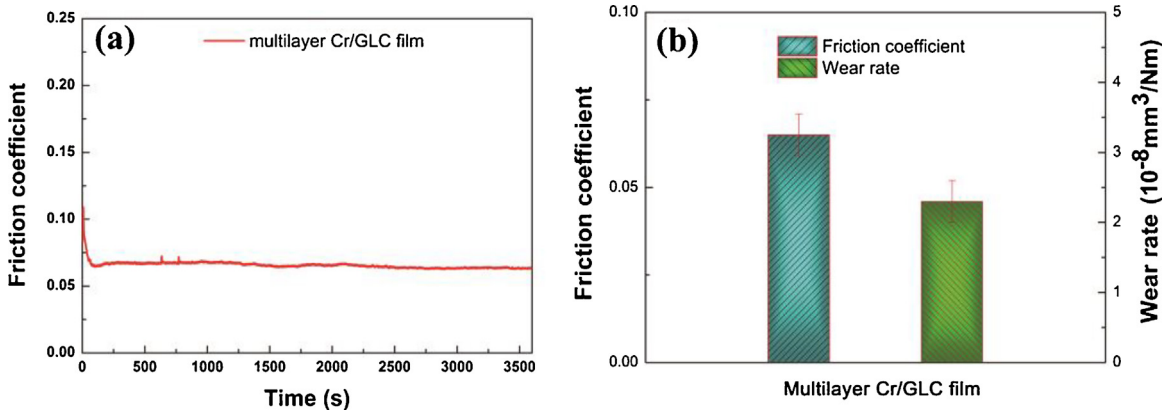

Fig. 9. (a) Friction coefficient curves of the multilayer Cr/GLC film sliding against a Si_3N_4 ball in artificial seawater and (b) The average friction coefficient and wear rate of the film.

the contact surface during tribo-process and will be discussed in Section 3.5.

The calculated wear rates are shown in Fig. 6(b). It is found that the average wear rate clearly increases from 6.0×10^{-8} to 28.1×10^{-8} mm^3/(N m) with increasing modulation ratio from 1:3 to 1:20. Additionally, the monolayer Cr/GLC film with modulation ratio of 1:3 shows the lowest wear rate, meaning that the lowest wear loss in seawater. Thus in the following part the monolayer Cr/GLC film with modulation ratio of 1:3 will be chosen as the representative to study wear behaviors.

Fig. 7(a) and (b) respectively shows SEM morphology and 2D profile of the wear track of the Cr/GLC film with the modulation ratio of 1:3 in seawater. It is clearly seen that the plough grooves and exfoliation area appear in the wear track, indicating that the material loss of the Cr/GLC film in seawater might result from local delamination. Overall, the wear track is wide and deep. From the EDS result shown in Fig. 7(c), the appearance of Fe signal evidences that the Cr/GLC film peeled from the substrate due to the synergistic effect of wear and corrosion in seawater. In consequence, the delamination is main factor to the durability of the Cr/GLC film on account of its great influence on wear failure in seawater.

3.4. Wear model of the Cr/GLC films in seawater

To analyze the tribological mechanism in seawater, the wear model of the Cr/GLC films in artificial seawater is depicted. Fig. 8 shows the propagation of defects area in seawater. In the initial stage, when the Cr/GLC films are sliding against Si3N4 balls in seawater, film defects may expand below the sliding surface. Under a few rounds of repeating sliding, seawater can infiltrate into the defects. The substrate elements close to defects are activated and bonds near the defects are seriously weakened [35]. In the second stage, because the Cl- can promote the dissolution of substrate, the metal can be dissolved to form metal ion in seawater. The formation of through-hole by defects propagation provides the channel of electron exchange in the process of substrate dissolving. Finally, the electrochemical reaction via electron exchange leads to the material loss. And the flaking of the Cr/GLC films will be intensified by wedging function from seawater penetrating into the defects. Eventually, the synergistic effect of wear and corrosion can substantially accelerate the failure and flaking off of the Cr/GLC film.

To analyze the tribological mechanism in seawater, the wear model of the Cr/GLC films in artificial seawater is depicted. Fig. 8 shows the expansion of defects area in seawater. In the initial stage, when the Cr/GLC films are sliding against Si_3N_4 balls in seawater, film defects may expand below the sliding surface. Under a few rounds of repeating sliding, seawater can infiltrate into the defects. The substrate elements close to defects are activated and Cl- can increase the dissolution of substrate in seawater [35]. In the second stage, the bonds near the defects are seriously weakened. Furthermore, the metal can dissolve to form metal ion in seawater. The formation of through-hole by defects expansion provides the channel of electron exchange. Finally, the electrochemical reaction via electron exchange leads to the material loss. And the flaking of the Cr/GLC films will be intensified by wedging function from seawater penetrating into the defects. Consequently, the synergistic effect

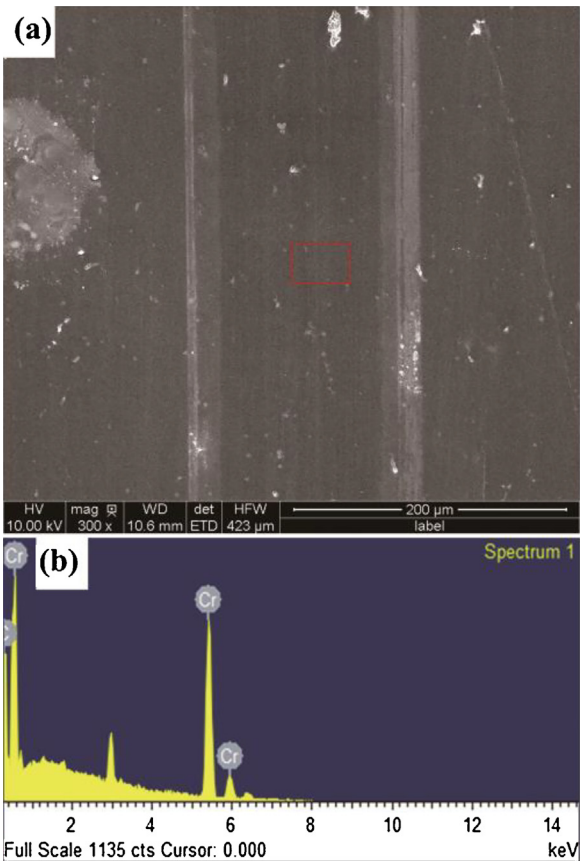

Fig. 10. Wear track of the multilayer Cr/GLC film with the modulation ratio of 1:3. (a) surface morphology, (b) EDS analysis.

of wear and corrosion can substantially accelerate the failure and flaking off of the Cr/GLC film.

3.5. *Effect of multilayer structure design on the tribological properties of the Cr/GLC films in seawater*

To further achieve high tribological performance in seawater, the multilayer structure Cr/GLC film is developed. Fig. S1 shows the cross-sectional microstructure of the multilayer structured Cr/GLC film. The film exhibits cyclical layer structure and has an overall thickness of ~1.0 μm. Fig. 9(a) shows the friction coefficient curve of the multilayer Cr/GLC film sliding against a Si_3N_4 ball in artificial seawater. Fig. 9(b) gives the average friction coefficient by averaging the values of the experimental data after 100 s and the wear rate calculated by Eq. (1). Furthermore, the potentiodynamic polarization tests were carried out to evaluate the corrosion resistance of the Cr/GLC films during sliding in seawater and the results are shown in Fig. S2. For 1:3 monolayer Cr/GLC film, i_{corr} is 4.8×10^{-9} A/cm^2, E_{corr} is −0.27 V. For 1:3 multilayer Cr/GLC film, i_{corr} is 3.2×10^{-9} A/cm^2, E_{corr} is −0.25 V. Obviously, the anti-corrosion property of the multilayer Cr/GLC film is superior to the monolayer Cr/GLC film, reflected by its lower corrosion current density (i_{corr}) and more positive corrosion potential (E_{corr}).

Fig. 10(a) shows the SEM morphology of wear track on the multilayer Cr/GLC film with modulation ratio of 1:3. Few flake pits are seen on the wear track. As seen from the EDS spectrum shown in Fig. 10(b), the signals of Cr and C elements can be detected easily in the friction region and the signal of Fe element is not detected, which suggests that the multilayer Cr/GLC film with modulation ratio of 1:3 possesses excellent tribological performance in corrosive environment. As analyzed before, the exfoliation pits are formed by the defects expansion. That is to say, the multilayer structure can prevent the formation of through-hole and limit the defects expansion.

In order to gain more insight into wear mechanisms of the Cr/GLC films, the 3D worn morphologies of coupled Si_3N_4 balls in seawater are shown in Fig. 11. Comparing the ball coupled with monolayer film, it can be found that the wear grooves on Si_3N_4 ball coupled with multilayer film are relatively smooth, which clearly demonstrates that the multilayer structure design is an effective measure to decrease friction, which generates less abrasion to the friction contact surfaces.

Also, the graphitization effect of tribo-films on the contact surfaces could reduce the friction and wear rate during tribo-test. Raman spectra obtained from the transferred tribo-films on wear scars of Si_3N_4 balls are shown in Fig. 12. It can be seen that the transferred tribo-films are formed on the Si_3N_4 balls and the broad bands range from 1000 to 1800 cm^{-1}, illustrating that the main content of the transferred tribo-film is carbonaceous feature [25]. Meanwhile, an obvious peak at approximately 1580 cm^{-1} can be found, which means that sp^2-hybridized carbon formed during sliding [36]. The

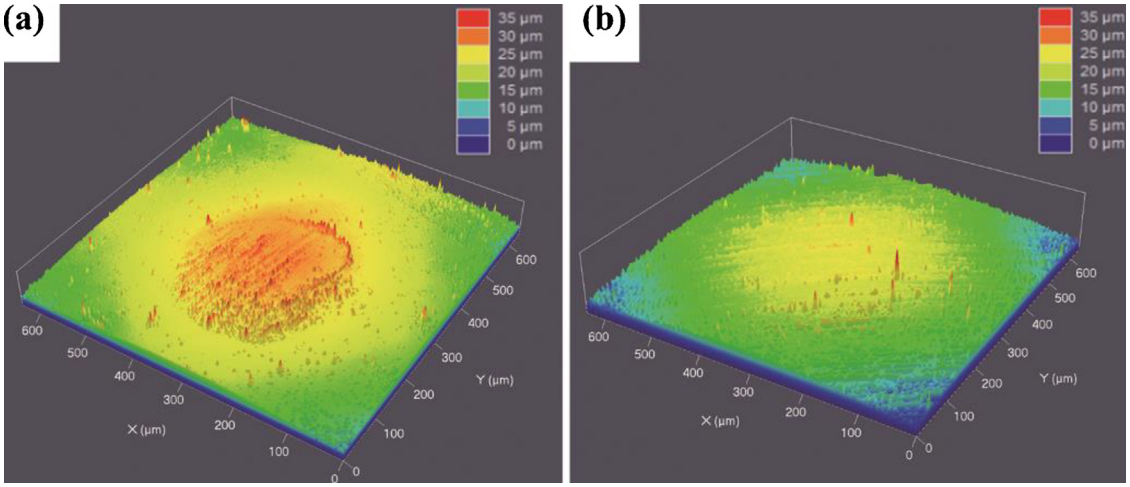

Fig. 11. 3-dimensional (3D) worn morphology of the ball in seawater friction tests with the film. (a) monolayer Cr/GLC film with the modulation ratio of 1:3, (b) multilayer Cr/GLC film with the modulation ratio of 1:3.

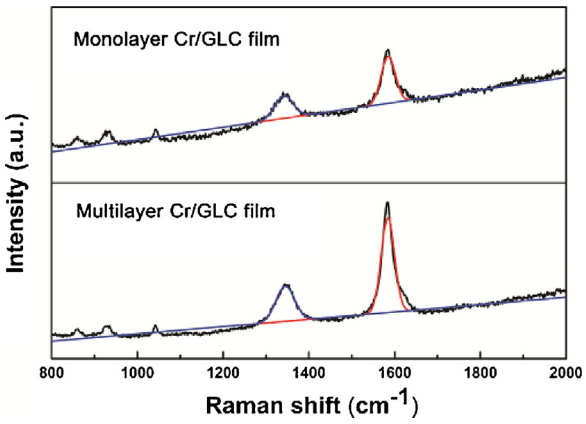

Fig. 12. Raman spectra of the transferred tribo-films on wear scars of Si_3N_4 balls.

intensity of G peak reflects the graphitization degree of the tribo-films. As shown, the intensity of G peak of the monolayer Cr/GLC film is obviously lower than that of the multilayer Cr/GLC film, indicating higher graphitization degree of the transferred tribo-films for the multilayer Cr/GLC film. The tribo-films can act as lubricant in sliding process and effectively reduce the friction and wear. Based on the above discussion, the synergistic effect of proper modulation ratio (1:3) and multilayer structure improves the tribological property of the Cr/GLC film, making it well applicable in the marine frictional components as a protective layer.

4. Conclusions

The Cr/GLC films with different Cr/GLC modulation ratios have been deposited by direct current magnetron sputtering technique. Through detailed characterization of the Gr/GLC films on structure, mechanical properties and tribological behaviors in artificial seawater, the main conclusions are summarized as follows:

1. With increasing the modulation ratio, the I_D/I_G and position (G) increase first and then decrease. When the modulation ratio is 1:3, the maximal values of I_D/I_G and G peak position reach 2.13 and 1549 cm^{-1}. However, the hardness and elastic modulus have the opposite variation trend and the lowest hardness and elastic modulus of (16.0 ± 0.7) GPa and (154.3 ± 9.8) GPa are obtained for the Cr/GLC film with modulation ratio of 1:3.
2. The Cr/GLC film with modulation ratio of 1:3 presents the lowest friction coefficient and wear rate, originating from its superiority of structure and mechanical properties.
3. The multilayer Cr/GLC film with modulation ratio of 1:3 exhibits the average friction coefficient of 0.08 ± 0.006 and the lowest wear rate of $(2.3 \pm 0.3) \times 10^{-8}$ $mm^3/(N\,m)$ in artificial seawater, confirming the proper modulation ratio (1:3) and optimized multilayer structure could prevent the formation of through-hole and limit the defects expansion.

Acknowledgments

The work was supported by the National Natural Science Foundation of China (Nos.51522106 and 51375475), Zhejiang Key Research and Development Program (2017C01001), and Public Projects of Zhejiang Province.

Appendix A. Supplementary data

Supplementary data associated with this article can be found, in the online version, at https://doi.org/10.1016/j.jmst.2017.12.002.

References

[1] Y. Ye, C. Wang, H. Chen, Y. Wang, J. Li, F. Ma, RSC Adv. 6 (2016) 32922–32931.
[2] L. Shan, Y. Wang, J. Li, X. Jiang, J. Chen, Tribol. Int. 82 (2015) 78–88.
[3] R.P.C. Costa, D.A. Lima-Oliveira, F.R. Marciano, A.O. Lobo, E.J. Corat, V.J. Trava-Airoldi, Appl. Surf. Sci. 285 (2013) 645–648.
[4] H. Hirani, S.S. Goilkar, Wear 266 (2009) 1141–1154.
[5] R.J.K. Wood, Wear 261 (2006) 1012–1023.
[6] K.H.Z. Gahr, M. Mathieu, B. Brylka, Wear 263 (2007) 920–929.
[7] M. Huang, X. Zhang, P. Ke, A. Wang, Appl. Surf. Sci. 283 (2013) 321–326.
[8] O. Knotek, F. Löffler, G. Krämer, Surf. Coat. Technol. 54–55 (1992) 241–248.
[9] Y. Ye, C. Wang, Y. Wang, W. Zhao, J. Li, Y. Yao, Surf. Coat. Technol. 280 (2015) 338–346.
[10] A.A. Voevodin, M.S. Donley, J.S. Zabinski, J.E. Bultman, Surf. Coat. Technol. 76 (1995) 534–539.
[11] Y. Wang, H. Li, L. Ji, X. Liu, Y. Wu, Y. Lv, Y. Fu, H. Zhou, J. Chen, J. Phys. D: Appl. Phys. 45 (2012) 556–563.
[12] M. Cui, J. Pu, J. Liang, L. Wang, G. Zhang, Q. Xue, RSC Adv. 5 (2015) 104829–104840.
[13] X. He, W. Li, H. Li, J. Vaccum Sci. Technol. A 14 (1996) 2039–2047.
[14] M. Kiuru, E. Alakoski, V.M. Tiainen, R. Lappalainen, A. Anttila, J. Biomed. Mater. Res. B 66 (2003) 425–428.
[15] Y. Wang, L. Wang, Q. Xue, Appl. Surf. Sci. 257 (2011) 4370–4376.
[16] W.Q. Bai, L.L. Li, Y.J. Xie, D.G. Liu, X.L. Wang, G. Jin, J.P. Tu, Surf. Coat. Technol. 305 (2016) 11–22.
[17] W. Zhang, A. Tanaka, B.S. Xu, Y. Koga, Diam. Relat. Mater. 14 (2005) 1361–1367.
[18] Y.S. Li, Y. Tang, Q. Yang, C. Xiao, A. Hirose, Appl. Surf. Sci. 256 (2010) 7653–7657.
[19] X. Guan, Z. Lu, L. Wang, Tribol. Lett. 44 (2011) 315–325.
[20] Y. Wang, J. Pu, J. Wang, J. Li, J. Chen, Q. Xue, Appl. Surf. Sci. 311 (2014) 816–824.
[21] J. Stallard, D. Mercs, M. Jarratt, D.G. Teer, P.H. Shipway, Surf. Coat. Technol. 177 (2004) 545–551.
[22] Z.M. Wang, J. Zhang, X. Han, Q.F. Li, Z.L. Wang, R. Wei, Corros. Sci. 86 (2014) 261–267.
[23] J.Z. Wang, F.Y. Yan, Q.J. Xue, Sci. Bull. 54 (2009) 4541–4548.
[24] J. Qi, L. Wang, Y. Wang, J. Pu, F. Yan, Q. Xue, Wear 271 (2011) 899–910.
[25] Y. Ye, C. Wang, H. Chen, Y. Wang, J. Li, F. Ma, RSC Adv. 6 (2016) 32922–32931.
[26] X. Chen, Z. Peng, X. Yu, Z. Fu, Y. Wen, C. Wang, Appl. Surf. Sci. 257 (2011) 3180–3186.
[27] A.C. Ferrari, J. Robertson, Phys. Rev. B: Condens. Matter. 61 (2000) 14095–14107.
[28] X. Li, P. Guo, L. Sun, X. Zuo, D. Zhang, P. Ke, A. Wang, Carbon 111 (2017) 467–475.
[29] X. Chen, Z. Peng, Z. Fu, W. Yue, X. Yu, C. Wang, Surf. Coat. Technol. 204 (2010) 3319–3325.
[30] K.M. Lee, H.J. Han, S. Choi, K.H. Park, J. Vac. Sci. Technol. B 21 (2003) 623–626.
[31] S.K. Field, M. Jarratt, D.G. Teer, Tribol. Int. 37 (2004) 949–956.
[32] Y. Wang, J. Pu, J. Wang, J. Li, J. Chen, Q. Xue, Appl. Surf. Sci. 311 (2014) 816–824.
[33] X. Zhang, Q. Huang, M. Liu, J. Tian, G. Zeng, Z. Li, K. Wang, Q. Zhang, Q. Wan, F. Deng, Appl. Surf. Sci. 343 (2015) 19–27.
[34] A. Leyland, A. Matthews, Wear 246 (2000) 1–11.
[35] S. Gao, C. Dong, L. Hong, K. Xiao, X. Pan, X. Li, Electrochim. Acta 114 (2013) 233–241.
[36] B. Vengudusamy, J.H. Green, G.D. Lamb, H.A. Spikes, Tribol. Int. 44 (2011) 165–174.